





# Mechanisms Mediating High-Molecular-Weight Hyaluronan-Induced Antihyperalgesia

Ivan J.M. Bonet,<sup>1</sup>  Dionéia Araldi,<sup>1</sup>  Eugen V. Khomula,<sup>1</sup> Oliver Bogen,<sup>1</sup>  Paul G. Green,<sup>2</sup> and  Jon D. Levine<sup>3</sup>

<sup>1</sup>Department of Oral and Maxillofacial Surgery, and Division of Neuroscience, University of California, San Francisco, San Francisco, California 94143, <sup>2</sup>Departments of Preventative and Restorative Dental Sciences and Oral and Maxillofacial Surgery, and Division of Neuroscience, University of California, San Francisco, San Francisco, California 94143, and <sup>3</sup>Departments of Medicine and Oral and Maxillofacial Surgery, and Division of Neuroscience, UCSF Pain and Addiction Research Center, University of California, San Francisco, San Francisco, California 94143

We evaluated the mechanism by which high-molecular-weight hyaluronan (HMWH) attenuates nociceptor sensitization, in the setting of inflammation. HMWH attenuated mechanical hyperalgesia induced by the inflammatory mediator prostaglandin E<sub>2</sub> (PGE<sub>2</sub>) in male and female rats. Intrathecal administration of an oligodeoxynucleotide antisense (AS-ODN) to mRNA for cluster of differentiation 44 (CD44), the cognate hyaluronan receptor, and intradermal administration of A5G27, a CD44 receptor antagonist, both attenuated antihyperalgesia induced by HMWH. In male rats, HMWH also signals via Toll-like receptor 4 (TLR4), and AS-ODN for TLR4 mRNA administered intrathecally, attenuated HMWH-induced antihyperalgesia. Since HMWH signaling is dependent on CD44 clustering in lipid rafts, we pretreated animals with methyl- $\beta$ -cyclodextrin (M $\beta$ CD), which disrupts lipid rafts. M $\beta$ CD markedly attenuated HMWH-induced antihyperalgesia. Inhibitors for components of intracellular signaling pathways activated by CD44, including phospholipase C and phosphoinositide 3-kinase (PI3K), also attenuated HMWH-induced antihyperalgesia. Furthermore, *in vitro* application of HMWH attenuated PGE<sub>2</sub>-induced sensitization of tetrodotoxin-resistant sodium current, in small-diameter dorsal root ganglion neurons, an effect that was attenuated by a PI3K inhibitor. Our results indicate a central role of CD44 signaling in HMWH-induced antihyperalgesia and suggest novel therapeutic targets, downstream of CD44, for the treatment of pain generated by nociceptor sensitization.

**Key words:** antihyperalgesia; cluster of differentiation 44 (CD44); high-molecular-weight hyaluronan (HMWH); hyaluronan; hyperalgesia; prostaglandin E<sub>2</sub> (PGE<sub>2</sub>)

## Significance Statement

High-molecular-weight-hyaluronan (HMWH) is used to treat osteoarthritis and other pain syndromes. In this study we demonstrate that attenuation of inflammatory hyperalgesia by HMWH is mediated by its action at cluster of differentiation 44 (CD44) and activation of its downstream signaling pathways, including RhoGTPases (RhoA and Rac1), phospholipases (phospholipases C $\epsilon$  and C $\gamma$ 1), and phosphoinositide 3-kinase, in nociceptors. These findings contribute to our understanding of the antihyperalgesic effect of HMWH and support the hypothesis that CD44 and its downstream signaling pathways represent novel therapeutic targets for the treatment of inflammatory pain.

## Introduction

Intra-articular high-molecular-weight hyaluronan (HMWH) is used clinically to treat osteoarthritis pain (Dougados et al., 1993;

Altman and Moskowitz, 1998; Cohen et al., 2008; Huang et al., 2011; Triantafyllidou et al., 2013). While it is generally considered that this therapeutic effect is mediated by its viscoelastic properties (Radin et al., 1970; Unsworth et al., 1975; Elmorsy et al., 2014; Cowman et al., 2015), recent evidence supports the suggestion that HMWH-induced antihyperalgesia is substantially related to its effects on nociceptor function (Gomis et al., 2007; Ferrari et al., 2016a, 2018). However, the mechanism by which HMWH produces antihyperalgesia remains poorly understood.

Hyaluronan (HA), a negatively charged linear polymer of a disaccharide composed of glucuronate and *N*-acetylglucosamine, is a major component of the extracellular matrix (Toole, 2009; Tavianatou et al., 2019). While HA is a simple repeating disaccharide, its biological effects are complex (Karousou et al., 2017;

Received Jan. 21, 2020; revised July 1, 2020; accepted July 4, 2020.

Author contributions: I.J.M.B., P.G.G., and J.D.L. designed research; I.J.M.B., D.A., E.V.K., and O.B. performed research; I.J.M.B., D.A., E.V.K., and O.B. analyzed data; I.J.M.B., D.A., E.V.K., O.B., P.G.G., and J.D.L. wrote the paper.

The authors declare no competing financial interests.

This study was funded by National Institutes of Health Grant AR-075334. We thank Monica Le and Samantha Stevens for technical assistance.

Correspondence should be addressed to Jon D. Levine at Jon.Levine@ucsf.edu.

<https://doi.org/10.1523/JNEUROSCI.0166-20.2020>

Copyright © 2020 the authors

Wight, 2017, 2018; Johnson et al., 2018). For example, HA can have different, and in some cases opposite, effects. For example, HA can be proinflammatory or anti-inflammatory, depending on its molecular weight (McKee et al., 1996; Yamawaki et al., 2009; Campo et al., 2010; Mizrahy et al., 2011; Kataoka et al., 2013; Furuta et al., 2017; Wu et al., 2018). We have suggested that low-molecular-weight HA (LMWH) and HMWH can act at nociceptors to produce prohyperalgesic and antihyperalgesic effects, respectively (Ferrari et al., 2018).

HMWH binds to and signals via several membrane receptors including, cluster of differentiation 44 (CD44), receptor for HA-mediated motility (RHAMM), and toll-like receptor 4 (TLR4; Vigetti et al., 2014; Tavianatou et al., 2019). The ability of HA to induce different CD44-dependent cell responses has been shown to be related to its molecular weight (Underhill, 1992; Tammi et al., 1998; Lesley et al., 2000; Louderbough and Schroeder, 2011; Padmanabhan and Gonzalez, 2012; Senbanjo and Chellaiah, 2017). For example, LMWH upregulates inflammation by stimulating the release of proinflammatory cytokines (McKee et al., 1996; Yamawaki et al., 2009; Campo et al., 2010), while HMWH is anti-inflammatory and immunosuppressant (Cuff et al., 2001; Mizrahy et al., 2011; Kataoka et al., 2013; Furuta et al., 2017; Wu et al., 2017). Further insight into the different effects of LMWH and HMWH has been provided by the observation that HMWH, but not LMWH, signaling is dependent on lipid rafts. For example, high levels of cholesterol promote CD44 translocation into lipid rafts, which is required for HMWH signaling via CD44 (Murai, 2015; Yang et al., 2018), while disrupting lipid rafts (Foger et al., 2001; Ito et al., 2004; Ghatak et al., 2005) suppresses HMWH-induced CD44 clustering in subsequent activation of downstream-dependent signaling (Bourguignon et al., 2000, 2003), and LMWH does not induce CD44 clustering (Yang et al., 2012). Previously, we demonstrated that HMWH markedly attenuated mechanical hyperalgesia induced by LMWH (Ferrari et al., 2016a), and by diverse pronociceptive inflammatory mediators in male rats, as well as paclitaxel chemotherapy-induced neuropathic pain (Ferrari et al., 2018). These observations suggest that elucidating the mechanism by which HMWH attenuates nociceptor sensitization could identify novel targets for the treatment of pain.

CD44, considered the cognate HA receptor (Bourguignon, 2014; Bourguignon et al., 2014), has been proposed to mediate the effects of HA on nociceptors (Ferrari et al., 2016a). In this study, we focus on the role of nociceptor CD44 and its downstream signaling pathways in the antihyperalgesia induced by HMWH, specifically the role of CD44 signaling molecules RhoA and Rac1, members of the Ras superfamily of small-molecular-weight GTPases (e.g., RhoA and Rac1), which act as molecular switches alternating between GTP-bound and GDP-bound states (Bourguignon et al., 2014), to in turn activate phosphoinositide 3-kinase (PI3K).

## Materials and Methods

**Animals.** All experiments were performed on female and male Sprague Dawley rats (weight, 220–400 g; Charles River Laboratories). Experimental animals were housed three per cage, under a 12 h light/dark cycle, in a temperature-controlled and humidity-controlled animal care facility of the University of California, San Francisco. Food and water were available *ad libitum*. Experimental protocols were approved by the Institutional Animal Care and Use Committee at the University of California, San Francisco, and adhered to the National Institutes of Health *Guidelines for the Care and Use of Laboratory Animals*. Effort was made to minimize the number of animals used and their suffering.

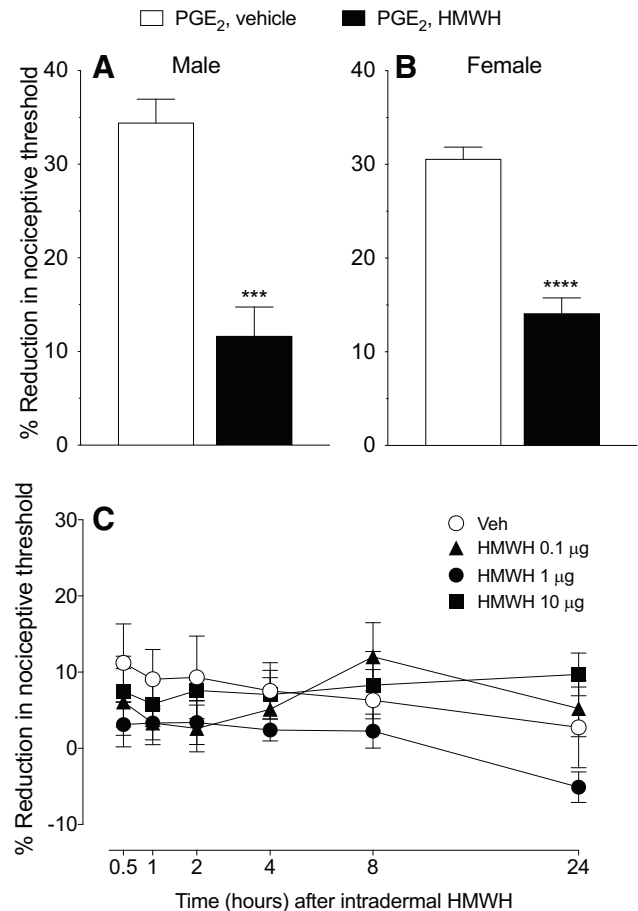


**Figure 1.** HMWH attenuates PGE<sub>2</sub> hyperalgesia but did not alone affect the nociceptive threshold. **A, B,** Male and female rats received PGE<sub>2</sub> (100 ng/5 μl, intradermally) on the dorsum of the hindpaw followed 10 min later by HMWH (1 μg/5 μl) or vehicle (5 μl) injected at the same site. The mechanical nociceptive threshold was then measured 40 min after intradermal PGE<sub>2</sub>. Measurement of mechanical nociceptive threshold showed a significant attenuation of PGE<sub>2</sub> hyperalgesia in rats treated with HMWH (**A**;  $t_{(10)} = 5.676$ ,  $***p = 0.0002$ , when the vehicle-treated group was compared with the HMWH-treated group; unpaired Student's *t* test; **B**;  $t_{(10)} = 7.860$ ,  $****p < 0.0001$ , when the vehicle-treated group was compared with the HMWH-treated group; unpaired Student's *t* test).  $n = 6$  paws in each group. **C,** Male rats received an intradermal injection of one of three doses of HMWH [0.1 μg, black triangle; 1 μg, black circle; or 10 μg, black square; diluted in 5 μl of saline] or vehicle (5 μl, white circle). Mechanical nociceptive threshold was evaluated 0.5, 1, 2, 4, 8, and 24 h after intradermal HMWH administration. The time course of the effect of HMWH on nociceptive threshold did not differ among the 0.1, 1, and 10 μg doses, and did not affect the nociceptive threshold itself. Repeated-measures two-way ANOVA, followed by Tukey's multiple-comparison test, revealed no significant interaction among the groups (interaction:  $F_{(15,100)} = 1.168$ ,  $p = 0.3088$ ; time:  $F_{(5,100)} = 1.241$ ,  $p = 0.2959$ ; dose:  $F_{(3,20)} = 1.093$ ,  $p = 0.3750$ ).  $n = 6$  paws in each group.

**Measuring nociceptive threshold.** Nociceptive testing was performed between 10:00 A.M. and 12:00 P.M., except for the experiments in Figure 1C, which were performed between 9:00 A.M. and 5:00 P.M. Mechanical nociceptive threshold was quantified using an Ugo Basile Analgesy-Meter (Stoelting), to perform the Randall–Selitto paw-withdrawal test. The Analgesy-Meter applies a linearly increasing mechanical force to the dorsum of the hindpaw of the rat, as previously described (Randall and Selitto, 1957; Taiwo et al., 1989; Taiwo and Levine, 1989). Rats were placed in cylindrical acrylic restrainers with lateral ports that allow extension of their hindlegs for nociceptive threshold testing, as previously described (Araldi et al., 2019), to acclimatize them to the experimental procedures.

Mechanical nociceptive threshold was defined as the force, in grams, at which the rat withdrew its paw. Baseline threshold was defined as the mean of three readings taken before the injection of test agents. Each experiment was performed on a different group of rats. Data are

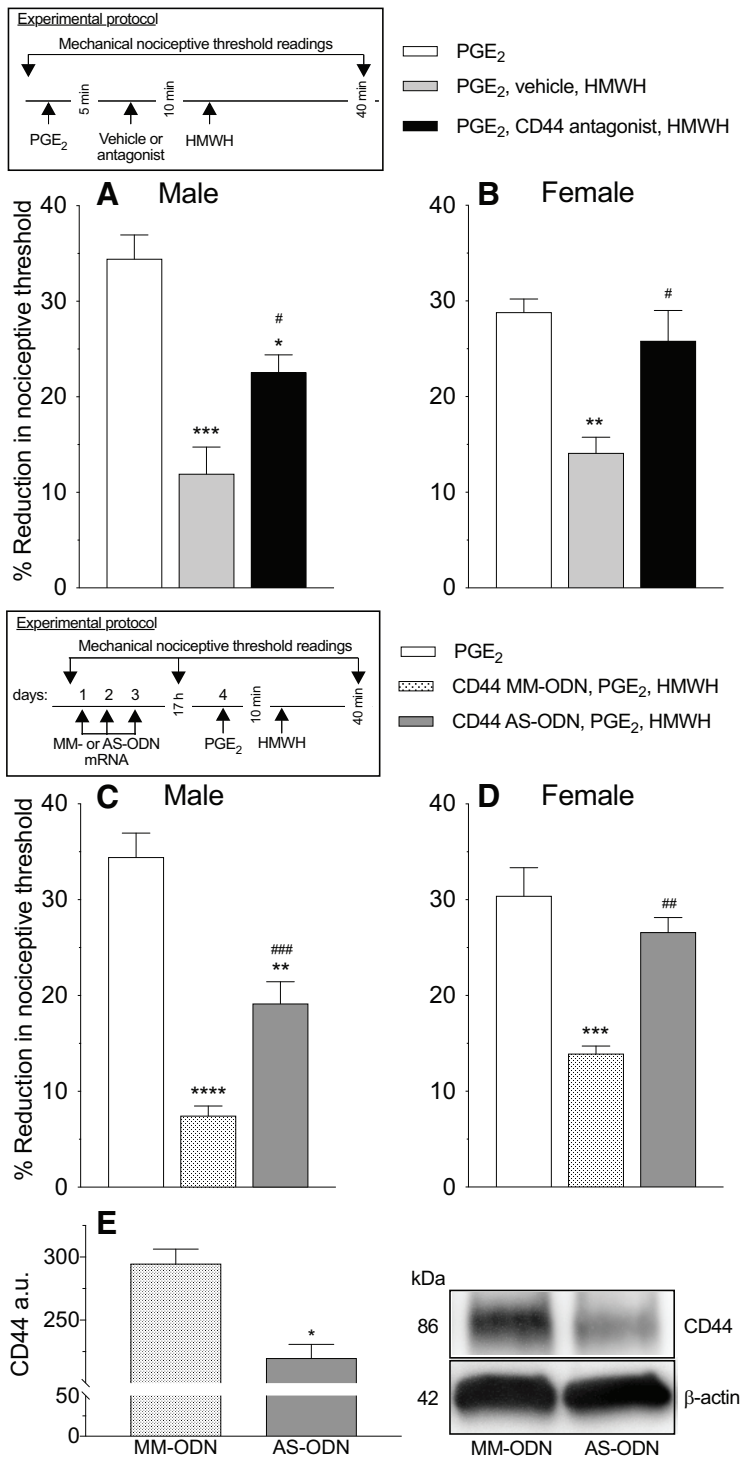


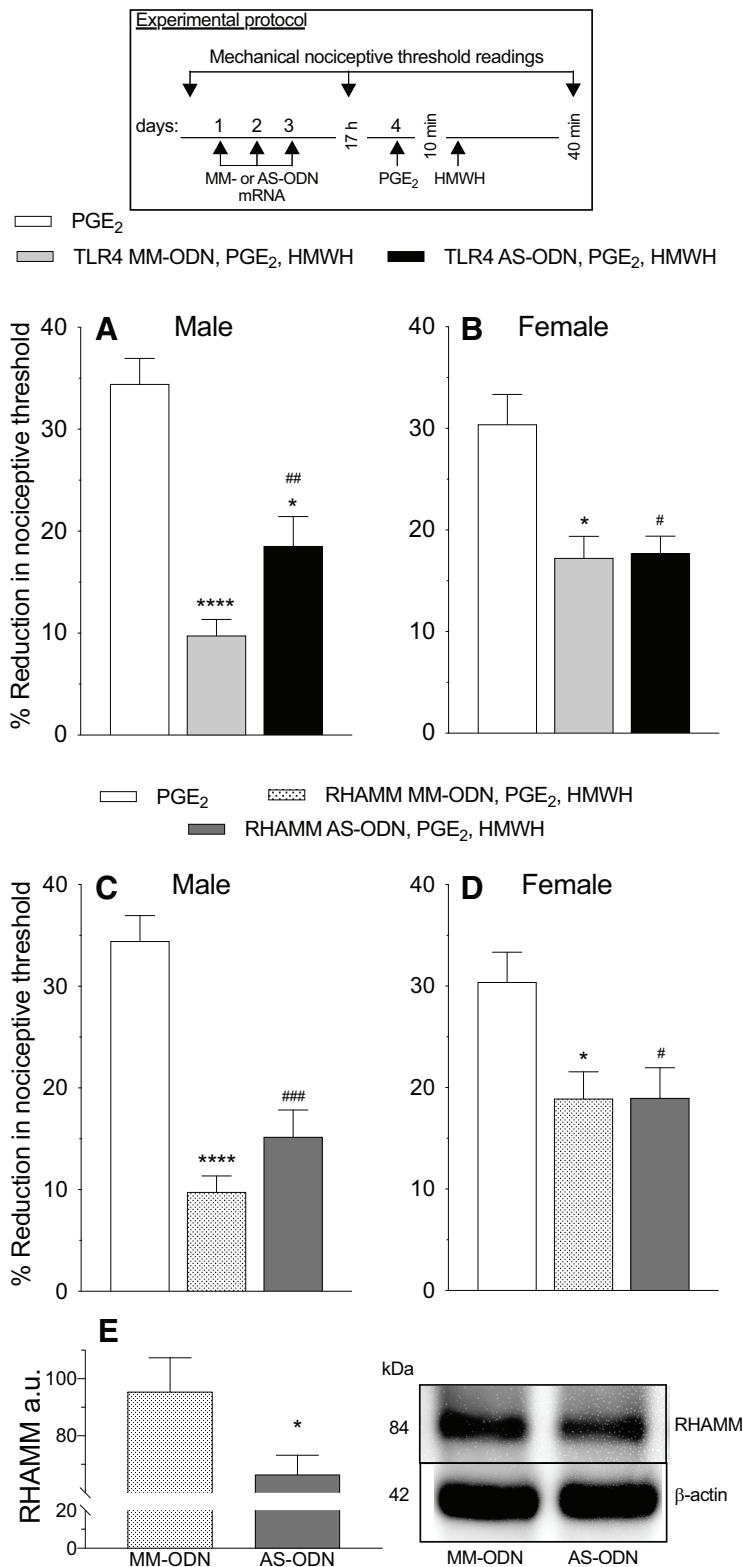
**Figure 2.** Reversal of PGE<sub>2</sub> hyperalgesia by HMWH was attenuated by CD44 ODN antisense and a CD44 receptor antagonist. **A, B**, Male and female rats were treated intradermally with PGE<sub>2</sub> (100 ng/2 μl), followed 5 min later by a CD44 receptor antagonist (A5G27, 1 μg/2 μl) or vehicle (2 μl) also injected intradermally. Ten minutes after PGE<sub>2</sub>, rats received intradermal HMWH (1 μg/2 μl) and the mechanical nociceptive threshold was evaluated before and 40 min after intradermal PGE<sub>2</sub>. In male rats that received a CD44 receptor antagonist, a significant attenuation in HMWH-induced antihyperalgesia was observed (**A**;  $F_{(2,10)} = 19.85$ ,  $\#p = 0.0344$ , when the CD44 receptor antagonist group plus the HMWH-treated group was compared with the vehicle group plus the HMWH-treated group;  $*p = 0.0191$ , when the CD44 receptor antagonist plus HMWH-treated group was compared with the PGE<sub>2</sub>-treated group alone;  $***p = 0.0002$ , when the vehicle group plus the HMWH-treated group was compared with PGE<sub>2</sub>-treated group alone 40 min after intradermal PGE<sub>2</sub> administration; two-way ANOVA followed by Tukey's multiple-comparisons test); however, in female rats HMWH-induced antihyperalgesia was completely reversed in the group that received CD44 antagonist receptor intradermally (**B**;  $F_{(2,10)} = 11.28$ ,  $\#p = 0.0127$ , when the CD44 receptor antagonist group plus the HMWH-treated group was compared with the vehicle group plus HMWH-treated group;  $***p = 0.0030$ , when the vehicle group plus the HMWH-treated group was compared with the PGE<sub>2</sub>-treated group

presented as the percentage change from baseline nociceptive threshold. Individuals performing the behavioral experiments (I.J.M.B. and D. A.) were blinded to interventions in the key experiments (Figs. 2, 3, 4, 5).

**Drugs.** The following drugs were used in this study: HMWH (hyaluronic acid sodium salt from *Streptococcus pyogenes*), from Calbiochem; prostaglandin E<sub>2</sub> (PGE<sub>2</sub>), methyl-β-cyclodextrin (MβCD), an Src inhibitor (SU6656), a MAPK/ERK inhibitor (U0126), PI3K inhibitors (wortmannin and LY294002), a phospholipase C (PLC) inhibitor (U73122), a Rho-associated kinase (ROK) inhibitor (Y27632), and a Rac1 inhibitor (NSC23766), all purchased from Sigma-Aldrich; and a CD44 antagonist (A5G27 [a peptide that binds to and inhibits CD44-dependent signaling]) from GenScript.

A stock solution of PGE<sub>2</sub>, dissolved in absolute ethanol to a concentration of 1 μg/μl, was further diluted in 0.9% NaCl, immediately before experiments. The ethanol concentration of the final PGE<sub>2</sub> solution was ~2%, a concentration previously shown to not affect the mechanical nociceptive threshold (Ferrari et al., 2016b).

alone 40 min after intradermal PGE<sub>2</sub> administration, two-way ANOVA followed by Tukey's multiple-comparisons test).  $n = 6$  paws in each group. **C, D**, Male and female rats were treated intrathecally with ODN AS or MM (120 μg/20 μl) for CD44 mRNA, daily for 3 consecutive days. On the fourth day, ~17 h after the last intrathecal administration of ODNs, PGE<sub>2</sub> (100 ng/5 μl) was injected intradermally on the dorsum of the hindpaw followed, 10 min later, by intradermal HMWH (1 μg/5 μl) or vehicle (5 μl). The mechanical nociceptive threshold was evaluated before and 40 min after intradermal PGE<sub>2</sub>. In male rats, the antihyperalgesic effect of HMWH on PGE<sub>2</sub>-induced hyperalgesia, was attenuated in the group treated with CD44 AS-ODN (**C**;  $F_{(2,10)} = 51.53$ ,  $###p = 0.0035$ , when the CD44 AS-ODN-treated group was compared with the CD44 ODN MM-treated group;  $**p < 0.0001$ , when the CD44 AS-ODN-treated group was compared with the PGE<sub>2</sub>-treated group alone,  $****p = 0.0002$ , when the CD44 MM-ODN-treated group was compared with the PGE<sub>2</sub>-treated group alone, 40 min after intradermal PGE<sub>2</sub>, two-way ANOVA followed by Tukey's multiple-comparisons test), while in female rats, CD44 AS-ODN completely reversed HMWH-induced antihyperalgesia (**D**;  $F_{(2,10)} = 18.23$ ,  $##p = 0.0033$ , when the CD44 AS-ODN-treated group is compared with CD44 MM-ODN-treated group;  $***p = 0.0005$ , when the CD44 MM-ODN-treated group was compared with the PGE<sub>2</sub>-treated group, 40 min after intradermal PGE<sub>2</sub>, two-way ANOVA followed by Tukey's multiple-comparisons test).  $n = 6$  paws each group. **E**, Western blot analysis of DRG extracts from male rats injected with 120 μg of CD44 AS-ODN/day for three consecutive days revealed a significant decrease in their anti-CD44 immunoreactivity when compared with the extracts derived from CD44 MM-ODN-treated rats ( $-24.8 \pm 4.8\%$ , unpaired Student's  $t$  test,  $n = 6$ ,  $p < 0.05$ ). The calculated molecular weight of the main CD44 splice variant in rat tissue is ~86 kDa (according to NCBI database entry NP\_037056). β-actin, which was used as a loading control, has a calculated molecular weight of ~42 kDa (according to UniProtKB database entry P60771).



Aliquots of HMWH, Y27632 and NSC23766, dissolved in distilled water to a concentration of 1 μg/μl, were further diluted in 0.9% NaCl to the concentration used in each experiment. Aliquots containing 1 μg/μl U0126, SU6656, U73122, LY249002, and wortmannin, dissolved in 100% dimethylsulfoxide (DMSO), were further diluted in 0.9% NaCl containing 10% DMSO to a concentration of 0.2 μg/μl.

All drugs were administered intradermally, in a volume of 5 μl (when injected alone) or 2 μl each (when two or more drugs are injected), on the dorsum of the hindpaw, using a 30 gauge hypodermic needle attached to a 50 μl Hamilton syringe by a segment of PE-10 polyethylene tubing from Becton Dickinson. The administration of NSC23766, Y27632, U0126, SU6656, U73122, LY249002, and wortmannin was preceded by a hypotonic shock (1 μl of distilled water, separated by a bubble of air to avoid mixing in the same syringe) to transiently facilitate enhanced cell permeability to these agents, to get reagents inside the nerve terminal (Borle and Snowdowne, 1982; Burch and Axelrod, 1987).

*Oligodeoxynucleotides antisense to CD44 receptor, Toll-like receptor 4, and RHAMM.* The role of CD44, Toll-like receptor 4

←

however, in female rats TLR4 AS-ODN did not affect the antihyperalgesia induced by HMWH (**B**;  $F_{(2,10)} = 8.051$ , #*p* = 0.0167 and \**p* = 0.0136, when the TLR4 AS-ODN- and TLR4 MM-ODN-treated group was compared with the PGE<sub>2</sub>-treated group alone; *p* = 0.9907, when TLR4 AS-ODN- and TLR4 MM-ODN-treated group are compared 40 min after intradermal PGE<sub>2</sub>, two-way ANOVA followed by Tukey's multiple-comparisons test). *n* = 6 paws each group. **C, D**, In male (**C**) and female (**D**) rats treated with RHAMM AS-ODN, the antihyperalgesia induced by HMWH was not affected (**C**;  $F_{(2,10)} = 43.23$ , ###*p* = 0.0001 and \*\*\*\**p* < 0.0001, when the RHAMM AS-ODN- and RHAMM MM-ODN-treated groups was compared with the PGE<sub>2</sub>-treated group alone; *p* = 0.1761, when the RHAMM AS-ODN- and MM-ODN-treated groups were compared each other, 40 min after intradermal PGE<sub>2</sub>, two-way ANOVA followed by Tukey's multiple-comparisons test. **D**;  $F_{(2,10)} = 6.043$ , #*p* < 0.0326 and \**p* = 0.0317, when the RHAMM AS-ODN-treated and RHAMM MM-ODN-treated groups was compared with the PGE<sub>2</sub>-treated group alone; *p* = 0.9998, when the RHAMM AS-ODN- and MM-ODN-treated groups were compared each other, 40 min after intradermal PGE<sub>2</sub> administration; two-way ANOVA followed by Tukey's multiple-comparisons test). *n* = 6 paws in each group. **E**, Western blot analysis of DRG extracts from male rats treated with 120 μg/day RHAMM AS ODN, for 3 consecutive days, reveals a significant decrease in RHAMM, compared with the extracts derived from RHAMM MM ODN-treated rats (−30.4 ± 4.6%, unpaired Student's *t* test, *n* = 6, \**p* = 0.0239). The calculated molecular weight of RHAMM is ~82.4 kDa (according to UniProtKB database entry Q9WUF7). β-actin, which was used as a loading control, has a calculated molecular weight of ~42 kDa (according to UniProtKB database entry P60771).

**Figure 3.** In male but not female rats, reversal of PGE<sub>2</sub> hyperalgesia by HMWH was TLR4 dependent. **A–D**, Male and female rats were treated intrathecally with AS-ODN (120 μg/20 μl) or MM-ODN (120 μg/20 μl) for TLR4 (**A, B**) or RHAMM (**C, D**) mRNA, once a day, for three consecutive days. On the fourth day, ~17 h after the last intrathecal administration of ODNs, PGE<sub>2</sub> (100 ng/5 μl) was injected intradermally on the dorsum of the hindpaw followed, 10 min later, by intradermal HMWH (1 μg/5 μl). The mechanical nociceptive threshold is evaluated 40 min after intradermal PGE<sub>2</sub>. **A, B**, In male rats treated with TLR4 AS-ODN an attenuation in the antihyperalgesia induced by HMWH was observed (**A**;  $F_{(2,10)} = 32.88$ , ##*p* = 0.0420, when the TLR4 AS-ODN-treated group was compared with TLR4 MM-ODN-treated group; \**p* < 0.001, when the TLR4 AS-ODN-treated group was compared with PGE<sub>2</sub>-treated group alone; \*\*\*\**p* < 0.0001, when the TLR4 MM-ODN-treated group was compared with the PGE<sub>2</sub>-treated group alone, 40 min after intradermal PGE<sub>2</sub>, two-way ANOVA followed by Tukey's multiple comparison test);



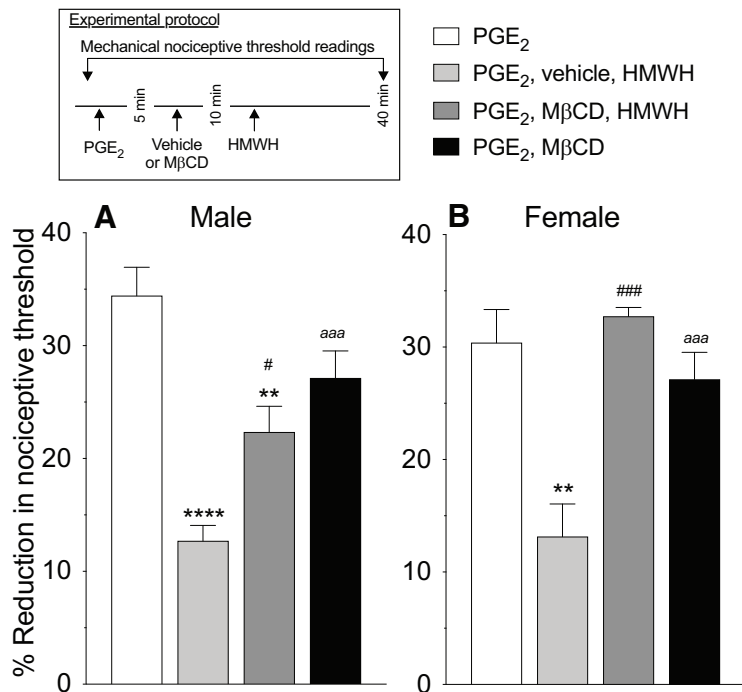


**Figure 4.** Lipid rafts are necessary for HMWH to induce antihyperalgesia. Male and female rats were treated intradermally with PGE<sub>2</sub> (100 ng/2 μl), followed 5 min later by a lipid raft disruptor (MβCD, 1 μg/2 μl) or vehicle (2 μl), also injected intradermally. Ten minutes after PGE<sub>2</sub> administration, rats received intradermal HMWH (1 μg/2 μl) and the mechanical nociceptive threshold was evaluated 40 min after intradermal PGE<sub>2</sub> administration. **A, Male:** MβCD significantly attenuated HMWH-induced antihyperalgesia ( $F_{(3,15)} = 22.60$ ,  $**p = 0.0023$ ,  $\#p = 0.0136$ , when the MβCD group plus the HMWH-treated group is compared with the PGE<sub>2</sub>-treated group and vehicle plus HMWH-treated group, respectively;  $****p < 0.0001$ , when the vehicle plus HMWH-treated group was compared with the PGE<sub>2</sub>-treated group, 40 min after intradermal PGE<sub>2</sub> administration;  $aaa p = 0.0004$ , when the MβCD-treated group was compared with the PGE<sub>2</sub>-treated group, 40 min after intradermal PGE<sub>2</sub> administration; two-way ANOVA followed by Tukey's multiple-comparisons test).  $n = 6$  paws in each group. **B, Female:** MβCD reverses HMWH-induced antihyperalgesia ( $F_{(3,15)} = 10.71$ ,  $###p = 0.0006$ , when the MβCD plus the HMWH-treated group was compared with the vehicle plus HMWH-treated group;  $**p = 0.0019$ , when the vehicle plus HMWH-treated group was compared with the PGE<sub>2</sub>-treated group;  $aaa p = 0.0004$ , when the MβCD-treated group was compared with the vehicle plus HMWH-treated group, 40 min after intradermal PGE<sub>2</sub>, two-way ANOVA followed by Tukey's multiple-comparisons test).  $n = 6$  paws in each group.

(TLR4), and RHAMM in the antihyperalgesic effects of HMWH was assessed in rats treated intrathecally with oligodeoxynucleotide (ODN) antisense (AS) to the mRNA of each receptor. All the AS-ODN sequences were directed against a unique region of the rat mRNA sequence for that receptor.

AS-ODN sequences were as follows: CD44 AS-ODN mRNA: 5'-GAA AAG GGT CGC GGG GG-3' (GenBank accession no. NM\_012924.2); TLR4 AS-ODN mRNA: 5'-AGG AAG TGA GAG TGC CAA CC-3' (GenBank accession no. NM\_019178.1); and RHAMM AS-ODN mRNA: 5'-ACC TGG AGA TGG AGC ACA AC-3' (GenBank accession no. NM\_012964.2).

Mismatch (MM) ODN sequences correspond to the antisense sequence with mismatched bases (denoted by bold letters). MM-ODN sequences were as follows: CD44 MM-ODN mRNA: 5'-CCC CCG CGA CCC TTT TC-3'; TLR4 MM-ODN mRNA: 5'-ACG ATG CGA GAG AGT CAC CG-3'; and RHAMM MM-ODN mRNA: 5'-GCC TGA AGA TAG ACG ACA AT-3'.

All ODNs were synthesized by Thermo Fisher Scientific; a decrease in TLR4 protein expression induced by the AS-ODN was recently demonstrated (Araldi et al., 2019). Before use, ODNs were reconstituted in nuclease-free 0.9% NaCl and then administered intrathecally at a dose of 6 μg/μl in a volume of 20 μl for 3 consecutive days (Araldi et al., 2019). As described previously (Alessandri-Haber et al., 2003), rats were anesthetized with isoflurane (2.5% in O<sub>2</sub>) and 120 μg of ODN, in a volume of 20 μl, injected intrathecally using a syringe attached to a 29 gauge needle inserted into the subarachnoid space, between the L4 and L5 vertebrae.

The intrathecal site of injection was confirmed by a sudden flick of the tail of the rat, a reflex that is evoked by subarachnoid space access and bolus intrathecal injection (Mestre et al., 1994). Animals regained consciousness ~2 min after the injection. The use of AS-ODN administered intrathecally to attenuate the expression of proteins, essential for their role in nociceptor sensitization, is well supported by previous studies conducted by others (Song et al., 2009; Su et al., 2011; Quanhong et al., 2012; Sun et al., 2013; Oliveira-Fusaro et al., 2017), as well as by our group (Parada et al., 2003; Bogen et al., 2012; Alvarez et al., 2014; Ferrari et al., 2016a,b, 2018; Araldi et al., 2017, 2019).

**SDS-PAGE and Western blotting.** Analysis of the efficacy of the antisense treatment for CD44 and RHAMM expression in male rat lumbar dorsal root ganglia (DRGs) was done by SDS-PAGE and Western blotting. Rats were killed by exsanguination, while under isoflurane anesthesia, 24 h after the last injection of antisense (or mismatch) ODN against CD44 or RHAMM mRNA. L4 and L5 DRGs were then surgically removed and stored at -80°C until further use. DRGs were transferred into homogenization buffer (100 mM NaCl, 1 mM EDTA, 2% SDS, 50 mM Tris-HCl, pH 7.4) that was supplemented with a protease inhibitor cocktail (Roche Diagnostics) and manually homogenized with a hand-held plastic pestle. Proteins were solubilized by incubating the homogenized DRGs for 2 h at 37°C, and homogenates were centrifuged at 1400 rpm in an Eppendorf Thermomixer. Solubilized proteins were extracted from insoluble cell and tissue components by a 15 min centrifugation at 14,000 rpm in an Eppendorf tabletop centrifuge. The protein concentrations of all samples were determined using the Pierce Micro BCA Protein Assay Kit (Thermo Fisher Scientific) with bovine serum albumin (BSA) as the standard. Mixtures of 40 μg of protein per sample were denatured by boiling in sample buffer [3% SDS, 10% (v/v) glycerol, 5% (v/v) β-mercaptoethanol, 0.025 mM bromophenol blue, and 62.5 mM Tris-HCl at pH 6.8] for 10 min, and were electrophoresed on 4–15% precast polyacrylamide gels (Bio-Rad) in 25 mM Tris containing 192 mM glycine and 0.1% SDS. Proteins were electrophoretically transferred to a nitrocellulose membrane using the semidry method [transfer time, 2 h at 60 mA/gel with 47.9 mM Tris, 38.9 mM glycine, 0.038% SDS and 20% (v/v) methanol].

The nitrocellulose membranes were saturated by shaking in antibody dilution buffer [5% BSA in Tris-buffered saline containing 0.1% Tween 20, at pH 7.4 (TBST)] for 1 h at room temperature (RT; 20–23°C), cut in half at ~50 kDa and probed with either a sheep polyclonal anti-CD44 antibody (1:500; catalog #AF6577, R&D Systems), a rabbit monoclonal anti-RHAMM (1:500; catalog #ab124729, Abcam), or a rabbit polyclonal anti-β-actin (1:1000; catalog #ab8227, Abcam) antibody in antibody dilution buffer at 4°C overnight. After rinsing with TBST (three times at RT, 15 min each), the RHAMM blot was probed with an biotinylated anti-rabbit antibody (1:2500; catalog #111-065-003, Jackson ImmunoResearch) for 2 h at RT, whereas the CD44 blot was probed with a horseradish peroxidase-conjugated anti-sheep antibody (1:2500 in antibody dilution buffer; R&D Systems) and the β-actin blots were probed with a horseradish peroxidase-conjugated anti-rabbit antibody (1:2500 in antibody dilution buffer; GE Healthcare LifeSciences) for 2 h at RT. All blotting membranes were rinsed with TBST (three times at RT, 15 min each), and the RHAMM blot was probed with a streptavidin-peroxidase polymer (1:5000; catalog #S2438, Sigma-Aldrich) for 1.5 h while shaking at RT. After rinsing with TBST (three times at RT, 15 min each), the immunoreactivities of all blots were visualized using the Pierce West Femto Chemiluminescence Detection System (Thermo Fisher Scientific). Results were analyzed using computer-assisted densitometry, and levels of CD44 or RHAMM immunoreactivity

were normalized with respect to the  $\beta$ -actin control levels in each sample. The percentage decrease in CD44 and RHAMM expression was calculated as follows: [(normalized density for AS/normalized density for MM  $\times$  100) – 100; Summer et al., 2008; Alvarez et al., 2017).

**Culture of DRG neurons.** Primary cultures of DRG neurons were made from adult male Sprague Dawley rats (weight, 220–235 g), as described previously (Ferrari et al., 2016b, 2018; Khomula et al., 2017, 2019; Araldi et al., 2019). In brief, under isoflurane anesthesia, rats were decapitated and the dorsum of the vertebral column surgically removed; L4 and L5 DRGs were rapidly extracted bilaterally, chilled, and desheathed in HBSS on ice. Ganglia were then treated with 0.25% collagenase type 4 (Worthington Biochemical) in HBSS for 18 min at 37°C, and then treated with 0.25% trypsin (Worthington Biochemical) in Invitrogen calcium-free and magnesium-free PBS (Thermo Fisher Scientific) for 6 min, followed by three washes and then trituration in Invitrogen Neurobasal-A medium (Thermo Fisher Scientific) to produce a single-cell suspension. This suspension was centrifuged at 1000 rpm for 3 min and resuspended in Neurobasal-A medium supplemented with 50 ng/ml nerve growth factor, 100 U/ml penicillin/streptomycin, B-27, GlutaMAX, and 10% FBS (Thermo Fisher Scientific). Cells were then plated on coverslips and incubated at 37°C in 3.5% CO<sub>2</sub> for at least 24 h before use in experiments.

**In vitro patch-clamp electrophysiology.** The bright-field imaging system consisted of an inverted microscope (Eclipse TE-200, Nikon Instruments) with an Andor Clara Interline CCD camera (Andor Technology), for high-resolution digital image acquisition, with MetaFluor software (Molecular Devices).

Cultured DRG neurons were used in *in vitro* electrophysiology experiments 24–96 h after DRG dissociation and plating neurons. While small-, medium-, and large-sized neurons were routinely observed in the same preparation, this study focused on cells with a soma diameter of <30  $\mu$ m (small DRG neurons), predominantly representing C-type nociceptors (Harper and Lawson, 1985; Woolf and Ma, 2007). After mounting a coverslip with cells in the recording chamber, the culture medium was replaced with the external perfusion solution containing the following (in mM): 100 TEA-Cl, 50 NaCl, 5 MgCl<sub>2</sub>, 0.1 CaCl<sub>2</sub>, 10 glucose, and 10 HEPES, and adjusted to pH 7.4 with TEA-OH; osmolarity is 310 mOsm/kg (Tuhkanen et al., 1998). Drugs were diluted to their final concentration in this solution. The volume of the recording chamber is 150  $\mu$ l. The perfusion system is gravity driven at a flow rate of 0.5–1 ml/min. All experiments were performed at RT.

Sodium currents in cultured DRG neurons were recorded in voltage-clamp mode of whole-cell patch clamp. Recording electrodes were fabricated from borosilicate glass capillaries [inner diameter (i.d.), 0.84 mm; outer diameter, 1.5 mm; Warner Instruments] using a Flaming/Brown P-87 puller (Sutter Instrument). Recording electrodes were filled with an intracellular perfusion solution containing the following (in mM): 100

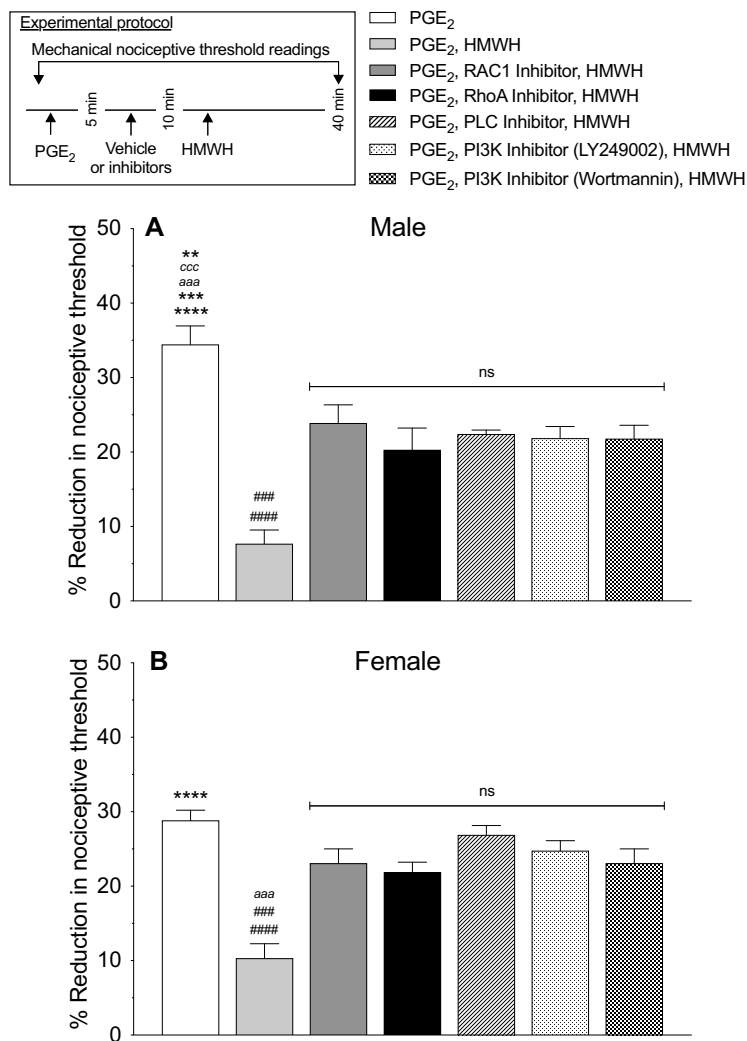


**Figure 5.** HMWH-induced antihyperalgesia is RhoA and Rac1 dependent. **A, B**, Male (**A**) and female (**B**) rats received PGE<sub>2</sub> (100 ng/2  $\mu$ l) intradermally followed 5 min later by intradermal vehicle (2  $\mu$ l), Rac1 inhibitor (NSC23766 1  $\mu$ g/2  $\mu$ l), RhoA inhibitor (Y27632 1  $\mu$ g/2  $\mu$ l), PLC inhibitor (U73122, 1  $\mu$ g/2  $\mu$ l), or PI3K inhibitors (wortmannin or LY249002, 1  $\mu$ g/2  $\mu$ l/each). Ten minutes after PGE<sub>2</sub> administration, rats received intradermal HMWH (1  $\mu$ g/2  $\mu$ l) and the mechanical nociceptive threshold was measured 40 min after intradermal PGE<sub>2</sub>. **A**, The antihyperalgesic effect of HMWH for PGE<sub>2</sub>-induced hyperalgesia was attenuated by second messenger inhibitors of the CD44 signaling pathways in male rats ( $F_{(6,30)} = 19.69$ ,  $####p < 0.0001$ , when the vehicle plus HMWH-treated group was compared with the NSC23766-, U73122-, LY249002-, and wortmannin-treated groups, respectively;  $###p = 0.0003$ , when the vehicle plus HMWH-treated group was compared with the Y27632-treated group;  $****p < 0.0001$ , when the PGE<sub>2</sub>-treated group was compared with the vehicle plus HMWH-treated and Y27632-treated groups, respectively;  $***p = 0.0003$ ,  $aaap = 0.0004$ ,  $cccp = 0.0003$ , and  $***p = 0.0034$ , when the PGE<sub>2</sub>-treated group was compared with the wortmannin-, LY249002-, U73122-, and NSC23766-treated groups, respectively, 40 min after intradermal PGE<sub>2</sub>; two-way ANOVA followed by Tukey's multiple-comparisons test).  $n = 6$  paws in each group. **B**, In female rats, an attenuation of the antihyperalgesic effect of HMWH for PGE<sub>2</sub>-induced hyperalgesia was observed in all groups treated with the second messenger inhibitors ( $F_{(6,30)} = 12.69$ ,  $####p < 0.0001$ , when the vehicle plus HMWH-treated group was compared with the LY249002- and U73122-treated groups, respectively;  $###p = 0.0001$ , when the vehicle plus HMWH-treated group was compared with the NSC23766 and wortmannin-treated groups, respectively;  $aaap = 0.0006$  when the vehicle plus HMWH-treated group was compared with Y27632-treated group;  $****p < 0.0001$ , when the PGE<sub>2</sub>-treated group is compared with the vehicle plus HMWH-treated group, 40 min after intradermal PGE<sub>2</sub> administration; two-way ANOVA followed by Tukey's multiple-comparisons test).  $n = 6$  paws in each group.

CsCl, 40 TEA-Cl, 2 MgCl<sub>2</sub>, 1 CaCl<sub>2</sub>, 10 EGTA, 5 MgATP, and 1 NaGTP, at pH 7.2 (adjusted with Tris base) and osmolarity at 300 mOsm. Junction potential was not adjusted. Recording electrode resistance was  $\sim 3.5$  M $\Omega$ . Series resistance was  $< 10$  M $\Omega$  at the end of recordings and was not compensated. Recordings were made with an Axon MultiClamp 700 B Amplifier, filtered at 10 kHz, and sampled at 20 kHz using an Axon Digidata 1550B digitizer controlled by pCLAMP 11 software (all from Molecular Devices). The holding membrane potential was set to  $-70$  mV. Tetrodotoxin-resistant (TTX-R) sodium current was induced

in the presence of TTX (100 nM) by voltage step to  $-10$  mV after 2 s conditioning at  $-50$  mV (Gold et al., 1998).

**Statistical analysis.** In all behavioral experiments, the dependent variable was the percentage change from baseline mechanical paw withdrawal threshold. We used 114 (186 paws) male rats and 96 (150 paws) female rats in the behavioral tests. In the experiments using AS- or MM-ODN for CD44 (Fig. 2), TLR4, and RHAMM (Fig. 3), we evaluated both paws. Repeated-measures two-way ANOVA followed by Tukey's multiple-comparisons test or Student's *t* test was used to analyze data.

Our Western blot results were presented as arbitrary units normalized to the reference protein  $\beta$ -actin. A total of 24 male rats (12 rats for CD44 AS-ODN and MM-ODN and 12 rats for RHAMM AS-ODN and MM-ODN mRNA) were used in Figures 2E and 3E. Differences between groups treated with AS-ODN and MM-ODN for CD44 and RHAMM mRNA were analyzed using an unpaired Student's *t* test.

In our electrophysiological experiments (see Fig. 7B), the dependent variable was the percentage reduction in peak sodium current induced by HMWH, relative to a baseline measured after stimulation with PGE<sub>2</sub>, in the absence or presence of PI3K inhibitor. Differences between two groups were analyzed using a two-tailed unpaired Student's *t* test (six neurons per group). A one-sample two-tailed Student's *t* test was used to compare the magnitude of the reduction to a theoretical value of 0% (for no change) to examine whether the effect of HMWH was statistically significant.

Prism version 8.0 (GraphPad Software) was used for the graphics and to perform statistical analyses;  $p < 0.05$  was considered statistically significant. Data are presented as the mean  $\pm$  SEM.

## Results

### HMWH attenuates PGE<sub>2</sub> hyperalgesia

We previously demonstrated that HMWH attenuates LMWH in male rats (Ferrari et al., 2016a). Here we first compare the effect of HMWH on PGE<sub>2</sub> hyperalgesia, in both sexes, and established its dose dependence. PGE<sub>2</sub> (100 ng) was administered intradermally, on the dorsum of the hindpaw, followed 10 min later by HMWH (1  $\mu$ g), injected at the same site. The mechanical nociceptive threshold was evaluated 40 min after intradermal PGE<sub>2</sub> administered. Hyperalgesia induced by PGE<sub>2</sub> was significantly attenuated by HMWH, in both male and female rats (Fig. 1A:  $t_{(10)} = 5.676$ ,  $p = 0.0002$ ; Fig. 1B:  $t_{(10)} = 7.860$ ,  $p < 0.0001$ , when the vehicle-treated and HMWH-treated groups are compared 40 min after intradermal PGE<sub>2</sub>, unpaired Student's *t* test). To exclude an independent effect on nociceptive threshold, we evaluated the effect of HMWH on baseline nociceptive threshold, in male rats. Three different doses of HMWH (0.1, 1, and 10  $\mu$ g) were administered intradermally on the dorsum of the hindpaw, in a volume of 5  $\mu$ l, and mechanical nociceptive threshold evaluated 0.5, 1, 2, 4, 8, and 24 h later. None of these doses of HMWH affected the nociceptive threshold (Fig. 1C:  $F_{(15,100)} = 1.168$ ,  $p = 0.3088$ , when the three different doses of HMWH are compared with the vehicle-treated group, 30 min after their injection; two-way ANOVA multiple-comparisons test). For subsequent experiments, we used the middle dose, 1  $\mu$ g, which we have previously shown to produce a robust antihyperalgesia (Ferrari et al., 2018).

### HMWH acts at CD44 to produce antihyperalgesia

To test the hypothesis that HMWH acts at CD44 to produce antihyperalgesia, rats received an intradermal injection of PGE<sub>2</sub> (100 ng) followed by injection of a CD44 antagonist (A5G27, 1  $\mu$ g) at the same site, and then 5 min later HMWH (1  $\mu$ g) was injected at the same site. Male rats receiving the CD44 antagonist showed attenuation of HMWH-induced anti-PGE<sub>2</sub> hyperalgesia (Fig. 2A;  $F_{(2,10)} = 19.85$ ,  $p = 0.0344$ , when the A5G27+HMWH-treated group is compared with vehicle+HMWH-treated group,

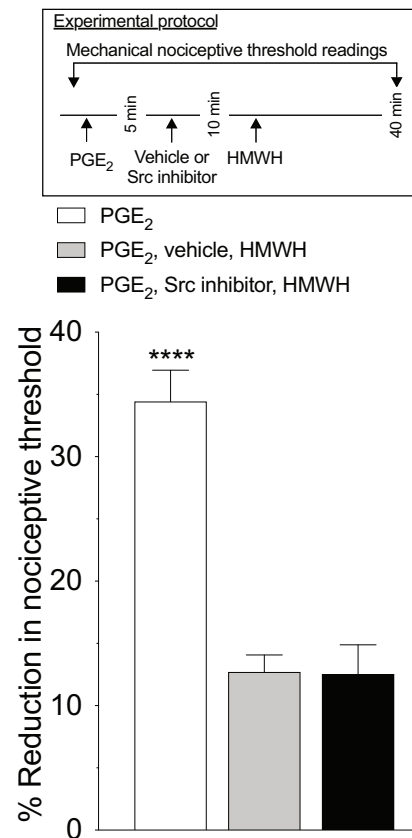


**Figure 6.** HMWH-induced antihyperalgesia is not dependent on Src. Male rats received an intradermal injection of PGE<sub>2</sub> (100 ng/2  $\mu$ l), followed 5 min later by the Src inhibitor (SU6656, 1  $\mu$ g/2  $\mu$ l) or vehicle (2  $\mu$ l), injected at the same site. Ten minutes after PGE<sub>2</sub> administration, rats received intradermal HMWH (1  $\mu$ g/2  $\mu$ l) and the mechanical nociceptive threshold was evaluated 40 min after intradermal PGE<sub>2</sub>. Treatment with the Src inhibitor SU6656 did not affect the antihyperalgesia induced by HMWH ( $F_{(2,10)} = 47.74$ ,  $****p < 0.0001$ , when the PGE<sub>2</sub>-treated group was compared with the vehicle plus HMWH-treated and SU6656-treated groups;  $p = 0.9979$ , when the SU6656-treated group is compared with the vehicle plus HMWH-treated group 40 min after intradermal PGE<sub>2</sub>; two-way ANOVA followed by Tukey's multiple-comparisons test).  $n = 6$  paws in each group.

40 min after intradermal PGE<sub>2</sub>; two-way ANOVA multiple-comparisons test). In female rats, the CD44 antagonist completely reversed HMWH-induced antihyperalgesia (Fig. 2B;  $F_{(2,10)} = 11.28$ ,  $p = 0.0127$ , when the A5G27+HMWH-treated group is compared with the vehicle+HMWH-treated group, 40 min after intradermal PGE<sub>2</sub>; two-way ANOVA multiple-comparisons test).

Additional groups of male and female rats received intrathecal AS-ODN for CD44 mRNA, daily for 3 consecutive days, as previously described (Ferrari et al., 2018). On the fourth day,  $\sim 17$  h after the last ODN administration, PGE<sub>2</sub> (100 ng) was injected intradermally on the dorsum of the hindpaw, followed 10 min later by HMWH (1  $\mu$ g) at the same site. In male rats that received CD44 AS-ODN, attenuation of HMWH-induced antihyperalgesia was observed (Fig. 2C;  $F_{(2,10)} = 51.53$ ,  $p = 0.0035$ , when the CD44 AS-ODN-treated group is compared with the CD44 MM-ODN-treated group, 40 min after intradermal PGE<sub>2</sub>, two-way ANOVA multiple-comparisons test), while in female rats, it was completely reversed (Fig. 2D;  $F_{(2,10)} = 18.23$ ,  $p = 0.0033$ , when the CD44 AS-ODN-treated and MM-ODN-treated groups are compared 40 min after intradermal PGE<sub>2</sub>; two-way ANOVA multiple-comparisons test).

Since HA also signals via RHAMM and TLR4 (Lennon and Singleton, 2011), we next evaluated whether the inhibition of



PGE<sub>2</sub> hyperalgesia by HMWH is RHAMM or TLR4 dependent. Rats received intrathecal administration of AS-ODN targeting RHAMM or TLR4 mRNA (Fig. 3). On the fourth day, ~17 h after the last intrathecal administration of ODN, PGE<sub>2</sub> (100 ng) was injected intradermally on the dorsum of the hindpaw, followed 10 min later by HMWH (1 μg) injected at the same site. In the group of male rats treated with TLR4 AS-ODN, an attenuation of HMWH-induced antihyperalgesia was observed (Fig. 3A;  $F_{(2,10)} = 32.88$ ,  $p = 0.0420$ , when the TLR4 AS-ODN-treated group is compared with TLR4 MM-ODN-treated group, 40 min after intradermal PGE<sub>2</sub>; two-way ANOVA multiple-comparisons test). However, intrathecal treatment with TLR4 AS-ODN did not affect HMWH-induced antihyperalgesia in female rats (Fig. 3B;  $F_{(2,10)} = 8.051$ ,  $p = 0.9907$ , when the TLR4 AS-ODN-treated and MM-ODN-treated groups are compared 40 min after intradermal PGE<sub>2</sub> administration; two-way ANOVA multiple-comparisons test). RHAMM AS-ODN did not affect the antihyperalgesic effect induced by HMWH in male or female rats (Fig. 3C:  $F_{(2,10)} = 43.23$ ,  $p = 0.1761$ , when the RHAMM AS-ODN-treated group was compared with MM-ODN-treated group, 40 min after intradermal PGE<sub>2</sub>; two-way ANOVA multiple-comparisons test; Fig. 3D:  $F_{(2,10)} = 6.043$ ,  $p = 0.9998$ , when the RHAMM AS-ODN-treated and MM-ODN-treated groups are compared 40 min after intradermal PGE<sub>2</sub>; two-way ANOVA multiple-comparisons test).

Previously, we demonstrated that TLR4 AS-ODN mRNA, administered intrathecally, reduced the expression of TLR4 in DRGs (Araldi et al., 2019). In the present study, we demonstrate knockdown of the expression of CD44 in DRGs by Western blot (pooled L4 and L5 ganglia) in ODN-treated male rats (Fig. 2E), in which we observed a  $24.8 \pm 4.8\%$  (arbitrary units normalized to the reference protein; unpaired Student's *t* test,  $p = 0.0005$ , when the CD44 AS-ODN-treated and MM-ODN-treated groups are compared; unpaired Student's *t* test) decrease in the expression of CD44 in DRGs from AS-ODN-treated rats, when compared with MM-ODN controls. Evidence for AS-ODN-induced reduction of RHAMM expression in DRGs can be seen in Western blots (pooled L4 and L5 ganglia) from ODN-treated male rats (Fig. 3E), in which we observe a  $30.4 \pm 4.6\%$  (arbitrary units normalized to the reference protein;  $p = 0.0306$ , when the RHAMM AS-ODN-treated and MM-ODN-treated groups are compared; unpaired Student's *t* test) decrease in the expression of RHAMM, in AS-ODN-treated rats, compared with the MM-ODN control.

#### Role of lipid rafts in HMWH-induced antihyperalgesia

Since signaling through CD44 and other HA receptors is lipid raft dependent, we investigated whether disrupting lipid rafts

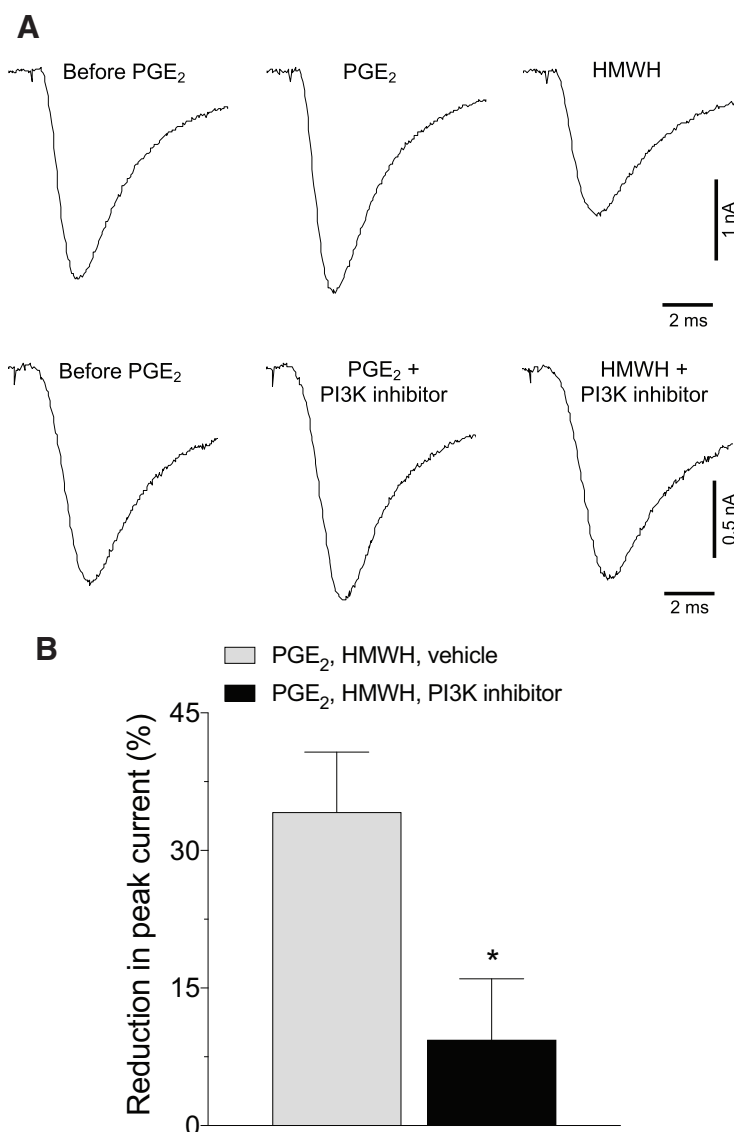


**Figure 7.** Inhibition of PI3K reverses attenuation of PGE<sub>2</sub>-sensitized TTX-R sodium current induced by HMWH. Small DRG neurons from male rats were held at  $-70$  mV in voltage-clamp mode of whole-cell patch clamp. TTX-R sodium current was induced in the presence of TTX (100 nM) by voltage step to  $-10$  mV after 2 s conditioning at  $-50$  mV. **A**, Illustrative traces depicting TTX-R sodium current as follows (left to right): before administration of PGE<sub>2</sub> (1 μM), 5 later, and 5 min after administration of HMWH (200 μg/ml) either alone (top) or with the addition of the PI3K inhibitor (LY249002, 50 μM; bottom). Note the substantial reduction in TTX-R sodium current induced by HMWH (top) and attenuation of this effect, when PI3K inhibitor was added (bottom). **B**, Pooled magnitudes of reduction in peak TTX-R sodium current 5 min after bath application of HMWH, relative to a baseline measured before this application (5 min after stimulation with 1 μM PGE<sub>2</sub>), in the absence (white bar) or presence (black bar) of PI3K inhibitor (LY249002, 50 μM). Inhibition of TTX-R sodium current by HMWH was attenuated by LY249002 (two-tailed unpaired Student's *t* test:  $t_{(10)} = 2.7$ ,  $*p = 0.024$ ).  $n = 6$  neurons/group.

attenuates HMWH-induced antihyperalgesia. Male and female rats were treated intradermally with PGE<sub>2</sub> (100 ng), followed 5 min later by MβCD (a lipid raft disruptor; 1 μg), and then a further 5 min later, HMWH was injected at the same site. We found that in male rats MβCD attenuates HMWH-induced antihyperalgesia (Fig. 4A;  $F_{(3,15)} = 22.60$ ,  $p = 0.0136$ , when the MβCD+HMWH-treated group was compared with the vehicle+HMWH-treated group 40 min after intradermal PGE<sub>2</sub>; two-way ANOVA multiple-comparisons test), while in female rats it was completely reversed (Fig. 4B;  $F_{(3,15)} = 10.71$ ,  $p = 0.0006$ , when the MβCD+HMWH-treated group was compared with the



vehicle+HMWH-treated group 40 min after intradermal PGE<sub>2</sub>; two-way ANOVA multiple-comparisons test).

### Second messengers mediating HMWH-induced antihyperalgesia

To evaluate for second messengers that mediate HMWH-induced antihyperalgesia, we screened second messengers for receptors implicated in HMWH signaling. To test the hypothesis that HMWH signals through RhoA or Rac1 to induce antihyperalgesia, male and female rats were treated intradermally with PGE<sub>2</sub> followed 5 min later by a Rac1 (NSC23766, 1 μg) or RhoA (Y27632, 1 μg) inhibitor and then, 5 min later, by HMWH (1 μg). All drugs were injected intradermally on the dorsum of the hind-paw. Male and female rats treated with NSC23766 or Y27632 show an attenuation of HMWH-induced antihyperalgesia (Fig. 5A:  $F_{(6,30)} = 19.69$ ,  $p < 0.0001$ , when the NSC23766+HMWH-treated group is compared with the vehicle+HMWH-treated group;  $p = 0.0003$ , when the Y23766+HMWH-treated group is compared with the vehicle+HMWH-treated group 40 min after intradermal PGE<sub>2</sub> administration; two-way ANOVA multiple-comparisons test; Fig. 5B:  $F_{(6,30)} = 12.69$ ,  $p = 0.0001$ , when the NSC23766+HMWH-treated group is compared with the vehicle+HMWH-treated group;  $p = 0.0006$ , when the Y23766+HMWH-treated group is compared with the vehicle+HMWH-treated group 40 min after intradermal PGE<sub>2</sub>; two-way ANOVA multiple-comparisons test).

RhoA and Rac1, in turn, activate ROK and PKN (fatty acid-activated serine/threonine kinase), respectively, which phosphorylate PLC $\epsilon$  and PLC $\gamma$ 1 (Bourguignon et al., 2014). To determine whether PLC is involved in HMWH-induced anti-PGE<sub>2</sub>-induced hyperalgesia, we treated male and female rats with PGE<sub>2</sub> intradermally, followed 5 min later by a PLC inhibitor (U73122, 1 μg), and then 5 min later by HMWH, also injected intradermally. In both male and female rats treated with U73122, HMWH-induced antihyperalgesia was attenuated (Fig. 5A:  $F_{(6,30)} = 19.69$ ,  $p < 0.0001$ , when the U73122+HMWH-treated group is compared with the vehicle+HMWH-treated group 40 min after intradermal PGE<sub>2</sub>; two-way ANOVA multiple-comparisons test; Fig. 5B:  $F_{(6,30)} = 12.69$ ,  $p = 0.0001$ , when the U73122+HMWH-treated group is compared with vehicle+HMWH-treated group 40 min after intradermal PGE<sub>2</sub>; two-way ANOVA multiple-comparisons test). The role of PI3K was also investigated, since RhoA activates ROK, which, in turn phosphorylates PLC $\epsilon$  and promotes the membrane localization of Gab-1 (scaffold protein), to activate PI3K (Bourguignon et al., 2014). Rats received PGE<sub>2</sub> intradermally, followed 5 min later by one of two PI3K inhibitors (wortmannin 1 μg or LY249002 1 μg), and then 5 min later by HMWH injected intradermally. In both male and female rats treated with either PI3K inhibitor, the antihyperalgesic effect induced by HMWH was attenuated (Fig. 5A:  $F_{(6,30)} = 19.69$ ,  $p < 0.0001$ , when the LY249002-treated and wortmannin+HMWH-treated groups are compared with the vehicle+HMWH-treated group, respectively, 40 min after intradermal PGE<sub>2</sub>; two-way ANOVA multiple-comparisons test; Fig. 5B:  $F_{(6,30)} = 19.69$ ,  $p < 0.0001$ ; and  $p = 0.0001$  when the LY249002-treated and wortmannin+HMWH-treated groups are compared with the vehicle+HMWH-treated group, respectively, 40 min after intradermal PGE<sub>2</sub>; two-way ANOVA multiple-comparisons test).

Finally, since Src is involved in LMWH-induced hyperalgesia (Ferrari et al., 2016a), we tested whether HMWH also signals through Src. Male rats were treated intradermally with PGE<sub>2</sub> followed 5 min later by an Src inhibitor (SU6656, 1 μg), and then 5 min later by HMWH. The Src inhibitor did not affect HMWH-induced antihyperalgesia (Fig. 6;  $F_{(2,10)} = 47.74$ ,  $p = 0.9979$ , when

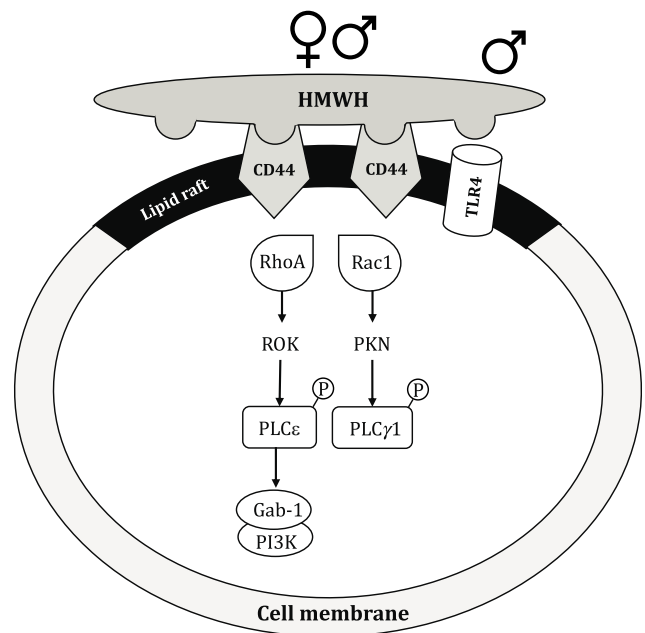


**Figure 8.** Schematic representation of potential signaling pathways involved in HMWH-induced antihyperalgesia. In male and female rats, HMWH binds to CD44 to induce its clustering in cell membrane lipid rafts and initiate signaling in downstream second messenger pathways. After HMWH binds to CD44, it can signal via RhoA and Rac1, which, in turn, activate ROK and PKN, respectively, leading to phosphorylation of PLC $\epsilon$  and PLC $\gamma$ 1, respectively. Binding of HMWH to CD44 also stimulates RhoA, which activates ROK to phosphorylate PLC $\epsilon$ , increasing serine/threonine phosphorylation of the adaptor protein Gab-1 and leading to activation of PI3K. In male rats, HMWH also signals via TLR4.

the SU6656+HMWH-treated group is compared with the vehicle+HMWH-treated group 40 min after intradermal PGE<sub>2</sub>; two-way ANOVA multiple-comparisons test).

Of note, all the inhibitors tested in this experiment were also injected intradermally, in groups pretreated 5 min before with intradermal PGE<sub>2</sub> (100 ng/2 μl). None of the inhibitors affected PGE<sub>2</sub>-induced hyperalgesia, measured 40 min after intradermal PGE<sub>2</sub> (data not shown).

### HMWH induces PI3K-dependent attenuation of PGE<sub>2</sub>-sensitized TTX-resistant sodium current *in vitro*

Potentiation of TTX-resistant voltage-gated sodium current (referred to here as TTX-R sodium current) contributes to a sensitizing effect of PGE<sub>2</sub>, reflected as a reduction in rheobase and in onset latency to action potential (Gold et al., 1998). We have recently shown that HMWH reverses PGE<sub>2</sub>-induced reduction in rheobase and action potential onset latency in cultured small DRG neurons (Ferrari et al., 2018). In the present experiments, we examined whether HMWH attenuates TTX-R sodium current in small DRG neurons from male rats sensitized by PGE<sub>2</sub> (England et al., 1996) and whether this is PI3K dependent. The peak magnitude of TTX-R sodium current recorded 5 min after administration of PGE<sub>2</sub> (1 μM) was considered as the baseline. HMWH (200 μg/ml) was then administered and 5 min later peak TTX-R sodium current measured, and its change relative to baseline analyzed (Fig. 7). HMWH significantly attenuated TTX-R sodium current, on average by  $34 \pm 7\%$  ( $n = 6$ ; compared with theoretical value of 0% with one-sample two-tailed Student's *t* test:  $t_{(5)} = 5.2$ ,  $p = 0.003$ ), supporting the suggestion that HMWH attenuates TTX-R sodium current, contributing to the antihyperalgesic effect of HMWH *in vivo*.

In our behavioral experiments, we found that the antihyperalgesic effect of HMWH is PI3K dependent (reversed to a similar extent by two PI3K inhibitors, LY249002 and wortmannin). Therefore, we next examined whether the prototypical PI3K inhibitor LY249002 can also reduce the attenuating effect of HMWH on PGE<sub>2</sub>-sensitized TTX-R sodium current. In a separate group of neurons, LY249002 (50 μM) was administered along with PGE<sub>2</sub> (1 μM) and then HMWH in the same above-mentioned protocol. We found that in the presence of LY249002, HMWH did not significantly attenuate TTX-R sodium current (the average reduction was only 9 ± 7%, *n* = 6; compared with 0% with the one-sample two-tailed Student's *t* test: *t*<sub>(5)</sub> = 1.4, *p* = 0.22). Attenuation of the effect of HMWH on TTX-R sodium current was significant (Fig. 7; eliminated ~75% of the initial effect; two-tailed unpaired Student's *t* test: *t*<sub>(10)</sub> = 2.7, *p* = 0.024; *n* = 6 neurons/group).

## Discussion

The fact that the receptor antagonist and AS-ODN for CD44 both inhibit HMWH-induced antihyperalgesia supports the suggestion that HMWH acts at CD44, present in nociceptors, to produce antihyperalgesia. That HMWH does not change mechanical nociceptive threshold in naive control rats, supports the suggestion that HMWH acts to reverse nociceptor sensitization. HA can also interact with other receptors, including TLR4 and RHAMM (Vigetti et al., 2014), and we found that TLR4 AS-ODN attenuated HMWH-induced antihyperalgesia only in male rats; and RHAMM AS-ODN did not affect HMWH-induced antihyperalgesia in either sex. The fact that in male, but not female, rats, HMWH-induced antihyperalgesia is partially dependent on TLR4 could be related to the ability of CD44 to act as a negative regulator of TLR4-mediated inflammation (Liang et al., 2007; Kawana et al., 2008); and that estrogen reduces TLR4 mRNA and protein by activation of the G-protein-coupled estrogen receptor (GPR30), which is significantly increased after ischemic injury (Zhang et al., 2018). Importantly, our results support the suggestion that CD44 is the major HA receptor at which HMWH acts to produce antihyperalgesia in females, while CD44 and TLR4 contribute to HMWH antihyperalgesia in males.

Since HMWH induces CD44 clustering, in lipid rafts, to regulate signaling (Donatello et al., 2012; Qian et al., 2012), we investigated whether disruption of lipid rafts could attenuate HMWH-induced antihyperalgesia. The lipid raft disruptor, MβCD, which alone does not affect PGE<sub>2</sub>-induced hyperalgesia, attenuates HMWH-induced antihyperalgesia. Our observation for dependence on lipid rafts for HMWH antihyperalgesia may be because of the requirement of CD44 clustering for HMWH, but not LMWH signaling (Lee et al., 2008; Wu et al., 2018). We cannot exclude the influence of other receptors, such as TLR4 in male rats, in the effect of MβCD, since the MβCD experiment was only meant to demonstrate the requirement of lipid rafts for HMWH-induced antihyperalgesia.

CD44 can also signal via RhoA and Rac1 (Bourguignon et al., 2014). Rats that received a Rac1 or RhoA inhibitor, demonstrated attenuation of HMWH-induced antihyperalgesia. RhoA and Rac1 activate ROK and PKN, respectively, which in turn phosphorylate PLCε and PLCγ1 (Bourguignon et al., 2014). We found that a PLC inhibitor also attenuated HMWH-induced antihyperalgesia. Furthermore, RhoA activates ROK to phosphorylate PLCε and promote the membrane localization of Gab-1, which, in turn, activates PI3K (Bourguignon et al., 2014). We

found that two PI3K inhibitors attenuated HMWH-induced antihyperalgesia. We also observed that the administration of HMWH significantly attenuated PGE<sub>2</sub>-sensitized TTX-R sodium current, in small-diameter DRG neurons. This effect was markedly reduced (~75%) by a PI3K inhibitor. These *in vitro* findings are in agreement with the results of our behavioral studies demonstrating PI3K-dependent reversal of PGE<sub>2</sub>-induced mechanical hyperalgesia following the administration of HMWH. Of note, PI3K inhibitors did not affect the mechanical nociceptive threshold or PGE<sub>2</sub>-induced hyperalgesia by themselves, excluding an independent role in the setting of nociceptive threshold or reversing hyperalgesia.

We cannot, at present, provide a mechanistic explanation of how PI3K can be both pronociceptive and antinociceptive (e.g., acting in different nociceptors or by a switch in downstream signaling pathways). Of note, however, there are several isoforms of PI3K, including different isoforms present in DRG (PI3Kα, PI3Kβ, PI3Kδ, and PI3Kγ; Leinders et al., 2014). And, different PI3K isoforms can execute distinct, and sometimes opposing, functions (Vanhaesebroeck et al., 2010). A second paradox relates to the activation of TLR4 (e.g., by lipopolysaccharide) to produce hyperalgesia (Wang et al., 2016), while we observed TLR4 mediating HMWH-induced antihyperalgesia in male rats. The ability of TLR4 AS-ODN to attenuate HMWH-induced antihyperalgesia, in males, could be because of a physical association between CD44 and TLR4 (Taylor et al., 2007). And, knocking down TLR4 expression may also decrease expression or functionality of CD44; the expression of CD44 in mesenchymal stem cells is lower in TLR4 knock-out mice (Wang et al., 2010).

CD44 induces changes in intracellular calcium in sensory neurons, increasing the excitability mediated by Src and focal adhesion kinase (Ghosh et al., 2011). While Src is involved in LMWH-induced hyperalgesia (Ferrari et al., 2016a), the Src inhibitor did not attenuate HMWH-induced antihyperalgesia.

The mechanisms by which HMWH antihyperalgesia is mediated in females by CD44, but not by TLR4 or RHAMM, has yet to be established. However, it is known that spinal TLR4 mediates hyperalgesia in male mice, but not in female mice, and while expression levels are not different, testosterone induces a switch in females to TLR4 dependence (Sorge et al., 2011).

We provide a schematic of the proposed signaling pathways that participate in HMWH-induced antihyperalgesia (Fig. 8). Our identification of a novel second messenger signaling pathway that reverses nociceptor sensitization opens a novel line of research into molecular targets for the treatment of pain syndromes that are dependent on nociceptor sensitization.

## References

- Alessandri-Haber N, Yeh JJ, Boyd AE, Parada CA, Chen X, Reichling DB, Levine JD (2003) Hypotonicity induces TRPV4-mediated nociception in rat. *Neuron* 39:497–511.
- Altman RD, Moskowitz R (1998) Intraarticular sodium hyaluronate (Hyalgan) in the treatment of patients with osteoarthritis of the knee: a randomized clinical trial. Hyalgan Study Group. *J Rheumatol* 25:2203–2212.
- Alvarez P, Green PG, Levine JD (2014) Role for monocyte chemoattractant protein-1 in the induction of chronic muscle pain in the rat. *Pain* 155:1161–1167.
- Alvarez P, Bogen O, Green PG, Levine JD (2017) Nociceptor interleukin 10 receptor 1 is critical for muscle analgesia induced by repeated bouts of eccentric exercise in the rat. *Pain* 158:1481–1488.
- Araldi D, Ferrari LF, Levine JD (2017) Hyperalgesic priming (type II) induced by repeated opioid exposure: maintenance mechanisms. *Pain* 158:1204–1216.

- Araldi D, Bogen O, Green PG, Levine JD (2019) Role of nociceptor Toll-like receptor 4 (TLR4) in opioid-induced hyperalgesia and hyperalgesic priming. *J Neurosci* 39:6414–6424.
- Bogen O, Alessandri-Haber N, Chu C, Gear RW, Levine JD (2012) Generation of a pain memory in the primary afferent nociceptor triggered by PKC $\epsilon$  activation of CPEB. *J Neurosci* 32:2018–2026.
- Borle AB, Snowdowne KW (1982) Measurement of intracellular free calcium in monkey kidney cells with aequorin. *Science* 217:252–254.
- Bourguignon LY (2014) Matrix hyaluronan-activated CD44 signaling promotes keratinocyte activities and improves abnormal epidermal functions. *Am J Pathol* 184:1912–1919.
- Bourguignon LY, Zhu H, Shao L, Chen YW (2000) CD44 interaction with tiam1 promotes Rac1 signaling and hyaluronic acid-mediated breast tumor cell migration. *J Biol Chem* 275:1829–1838.
- Bourguignon LY, Singleton PA, Zhu H, Diedrich F (2003) Hyaluronan-mediated CD44 interaction with RhoGEF and Rho kinase promotes Grb2-associated binder-1 phosphorylation and phosphatidylinositol 3-kinase signaling leading to cytokine (macrophage-colony stimulating factor) production and breast tumor progression. *J Biol Chem* 278:29420–29434.
- Bourguignon LY, Shiina M, Li JJ (2014) Hyaluronan-CD44 interaction promotes oncogenic signaling, microRNA functions, chemoresistance, and radiation resistance in cancer stem cells leading to tumor progression. *Adv Cancer Res* 123:255–275.
- Burch RM, Axelrod J (1987) Dissociation of bradykinin-induced prostaglandin formation from phosphatidylinositol turnover in Swiss 3T3 fibroblasts: evidence for G protein regulation of phospholipase A2. *Proc Natl Acad Sci U S A* 84:6374–6378.
- Campo GM, Avenoso A, Campo S, D'Ascola A, Nastasi G, Calatroni A (2010) Small hyaluronan oligosaccharides induce inflammation by engaging both toll-like-4 and CD44 receptors in human chondrocytes. *Biochem Pharmacol* 80:480–490.
- Cohen MM, Altman RD, Hollstrom R, Hollstrom C, Sun C, Gipson B (2008) Safety and efficacy of intra-articular sodium hyaluronate (Hyalgan) in a randomized, double-blind study for osteoarthritis of the ankle. *Foot Ankle Int* 29:657–663.
- Cowman MK, Schmidt TA, Raghavan P, Stecco A (2015) Viscoelastic properties of hyaluronan in physiological conditions. *F1000Res* 4:622.
- Cuff CA, Kothapalli D, Azonobi I, Chun S, Zhang Y, Belkin R, Yeh C, Secreto A, Assoian RK, Rader DJ, Puré E (2001) The adhesion receptor CD44 promotes atherosclerosis by mediating inflammatory cell recruitment and vascular cell activation. *J Clin Invest* 108:1031–1040.
- Donatello S, Babina IS, Hazelwood LD, Hill AD, Nabi IR, Hopkins AM (2012) Lipid raft association restricts CD44-ezrin interaction and promotion of breast cancer cell migration. *Am J Pathol* 181:2172–2187.
- Dougados M, Nguyen M, Listrat V, Amor B (1993) High molecular weight sodium hyaluronate (hyalectin) in osteoarthritis of the knee: a 1 year placebo-controlled trial. *Osteoarthritis Cartil* 1:97–103.
- Elmorsy S, Funakoshi T, Sasazawa F, Todoh M, Tadano S, Iwasaki N (2014) Chondroprotective effects of high-molecular-weight cross-linked hyaluronic acid in a rabbit knee osteoarthritis model. *Osteoarthritis Cartilage* 22:121–127.
- England S, Bevan S, Docherty RJ (1996) PGE2 modulates the tetrodotoxin-resistant sodium current in neonatal rat dorsal root ganglion neurons via the cyclic AMP-protein kinase A cascade. *J Physiol* 495:429–440.
- Ferrari LF, Araldi D, Bogen O, Levine JD (2016a) Extracellular matrix hyaluronan signals via its CD44 receptor in the increased responsiveness to mechanical stimulation. *Neuroscience* 324:390–398.
- Ferrari LF, Khomula EV, Araldi D, Levine JD (2016b) Marked sexual dimorphism in the role of the ryanodine receptor in a model of pain chronification in the rat. *Sci Rep* 6:31221.
- Ferrari LF, Khomula EV, Araldi D, Levine JD (2018) CD44 signaling mediates high molecular weight hyaluronan-induced antihyperalgesia. *J Neurosci* 38:308–321.
- Foger N, Marhaba R, Zoller M (2001) Involvement of CD44 in cytoskeleton rearrangement and raft reorganization in T cells. *J Cell Sci* 114:1169–1178.
- Furuta J, Ariyoshi W, Okinaga T, Takeuchi J, Mitsugi S, Tominaga K, Nishihara T (2017) High molecular weight hyaluronic acid regulates MMP13 expression in chondrocytes via DUSP10/MKP5. *J Orthop Res* 35:331–339.
- Ghatak S, Misra S, Toole BP (2005) Hyaluronan constitutively regulates ErbB2 phosphorylation and signaling complex formation in carcinoma cells. *J Biol Chem* 280:8875–8883.
- Ghosh B, Li Y, Thayer SA (2011) Inhibition of the plasma membrane Ca<sup>2+</sup> pump by CD44 receptor activation of tyrosine kinases increases the action potential afterhyperpolarization in sensory neurons. *J Neurosci* 31:2361–2370.
- Gold MS, Levine JD, Correa AM (1998) Modulation of TTX-R INa by PKC and PKA and their role in PGE2-induced sensitization of rat sensory neurons *in vitro*. *J Neurosci* 18:10345–10355.
- Gomis A, Miralles A, Schmidt RF, Belmonte C (2007) Nociceptive nerve activity in an experimental model of knee joint osteoarthritis of the guinea pig: effect of intra-articular hyaluronan application. *Pain* 130:126–136.
- Harper AA, Lawson SN (1985) Conduction velocity is related to morphological cell type in rat dorsal root ganglion neurons. *J Physiol* 359:31–46.
- Huang TL, Chang CC, Lee CH, Chen SC, Lai CH, Tsai CL (2011) Intra-articular injections of sodium hyaluronate (Hyalgan(R)) in osteoarthritis of the knee. a randomized, controlled, double-blind, multicenter trial in the Asian population. *BMC Musculoskelet Disord* 12:221.
- Ito T, Williams JD, Fraser DJ, Phillips AO (2004) Hyaluronan regulates transforming growth factor-beta1 receptor compartmentalization. *J Biol Chem* 279:25326–25332.
- Johnson P, Arif AA, Lee-Sayer SSM, Dong Y (2018) Hyaluronan and its interactions with immune cells in the healthy and inflamed lung. *Front Immunol* 9:2787.
- Karousou E, Misra S, Ghatak S, Dobra K, Götte M, Vigetti D, Passi A, Karamanos NK, Skandalis SS (2017) Roles and targeting of the HAS/hyaluronan/CD44 molecular system in cancer. *Matrix Biol* 59:3–22.
- Kataoka Y, Ariyoshi W, Okinaga T, Kaneuji T, Mitsugi S, Takahashi T, Nishihara T (2013) Mechanisms involved in suppression of ADAMTS4 expression in synoviocytes by high molecular weight hyaluronic acid. *Biochem Biophys Res Commun* 432:580–585.
- Kawana H, Karaki H, Higashi M, Miyazaki M, Hilberg F, Kitagawa M, Harigaya K (2008) CD44 suppresses TLR-mediated inflammation. *J Immunol* 180:4235–4245.
- Khomula EV, Ferrari LF, Araldi D, Levine JD (2017) Sexual dimorphism in a reciprocal interaction of ryanodine and IP3 receptors in the induction of hyperalgesic priming. *J Neurosci* 37:2032–2044.
- Khomula EV, Araldi D, Levine JD (2019) *In vitro* nociceptor neuroplasticity associated with *in vivo* opioid-induced hyperalgesia. *J Neurosci* 39:7061–7073.
- Lee JL, Wang MJ, Sudhir PR, Chen JY (2008) CD44 engagement promotes matrix-derived survival through the CD44-SRC-integrin axis in lipid rafts. *Mol Cell Biol* 28:5710–5723.
- Leinders M, Koehrn FJ, Bartok B, Boyle DL, Shubayev V, Kalcheva I, Yu NK, Park J, Kaang BK, Hefferan MP, Firestein GS, Sorkin LS (2014) Differential distribution of PI3K isoforms in spinal cord and dorsal root ganglia: potential roles in acute inflammatory pain. *Pain* 155:1150–1160.
- Lennon FE, Singleton PA (2011) Role of hyaluronan and hyaluronan-binding proteins in lung pathobiology. *Am J Physiol Lung Cell Mol Physiol* 301:L137–L147.
- Lesley J, Hascall VC, Tammi M, Hyman R (2000) Hyaluronan binding by cell surface CD44. *J Biol Chem* 275:26967–26975.
- Liang J, Jiang D, Griffith J, Yu S, Fan J, Zhao X, Bucala R, Noble PW (2007) CD44 is a negative regulator of acute pulmonary inflammation and lipopolysaccharide-TLR signaling in mouse macrophages. *J Immunol* 178:2469–2475.
- Louderbough JM, Schroeder JA (2011) Understanding the dual nature of CD44 in breast cancer progression. *Mol Cancer Res* 9:1573–1586.
- McKee CM, Penno MB, Cowman M, Burdick MD, Strieter RM, Bao C, Noble PW (1996) Hyaluronan (HA) fragments induce chemokine gene expression in alveolar macrophages. The role of HA size and CD44. *J Clin Invest* 98:2403–2413.
- Mestre C, Pélissier T, Fialip J, Wilcox G, Eschalié A (1994) A method to perform direct transcutaneous intrathecal injection in rats. *J Pharmacol Toxicol Methods* 32:197–200.
- Mizrahy S, Raz SR, Hasgaard M, Liu H, Soffer-Tsur N, Cohen K, Dvash R, Landsman-Milo D, Bremer MG, Moghimi SM, Peer D (2011) Hyaluronan-coated nanoparticles: the influence of the molecular weight on CD44-hyaluronan interactions and on the immune response. *J Control Release* 156:231–238.



- Murai T (2015) Lipid raft-mediated regulation of hyaluronan-CD44 interactions in inflammation and cancer. *Front Immunol* 6:420.
- Oliveira-Fusaro MCG, Zanoni CIS, Dos Santos GG, Manzo LP, Araldi D, Bonet IJM, Tambeli CH, Dias EV, Parada CA (2017) Antihyperalgesic effect of CB1 receptor activation involves the modulation of P2X3 receptor in the primary afferent neuron. *Eur J Pharmacol* 798:113–121.
- Padmanabhan J, Gonzalez AL (2012) The effects of extracellular matrix proteins on neutrophil-endothelial interaction—a roadway to multiple therapeutic opportunities. *Yale J Biol Med* 85:167–185.
- Parada CA, Yeh JJ, Reichling DB, Levine JD (2003) Transient attenuation of protein kinase C $\epsilon$  can terminate a chronic hyperalgesic state in the rat. *Neuroscience* 120:219–226.
- Qian H, Xia L, Ling P, Waxman S, Jing Y (2012) CD44 ligation with A3D8 antibody induces apoptosis in acute myeloid leukemia cells through binding to CD44s and clustering lipid rafts. *Cancer Biol Ther* 13:1276–1283.
- Quanhong Z, Ying X, Moxi C, Tao X, Jing W, Xin Z, Li W, Derong C, Xiaoli Z, Wei J (2012) Intrathecal PLC( $\beta$ 3) oligodeoxynucleotides antisense potentiates acute morphine efficacy and attenuates chronic morphine tolerance. *Brain Res* 1472:38–44.
- Radin EL, Swann DA, Weisser PA (1970) Separation of a hyaluronate-free lubricating fraction from synovial fluid. *Nature* 228:377–378.
- Randall LO, Selitto JJ (1957) A method for measurement of analgesic activity on inflamed tissue. *Arch Int Pharmacodyn Ther* 111:409–419.
- Senbanjo LT, Chellaiah MA (2017) CD44: a multifunctional cell surface adhesion receptor is a regulator of progression and metastasis of cancer cells. *Front Cell Dev Biol* 5:18.
- Song MJ, Wang YQ, Wu GC (2009) Additive anti-hyperalgesia of electroacupuncture and intrathecal antisense oligodeoxynucleotide to interleukin-1 receptor type I on carrageenan-induced inflammatory pain in rats. *Brain Res Bull* 78:335–341.
- Sorge RE, LaCroix-Fralish ML, Tuttle AH, Sotocinal SG, Austin JS, Ritchie J, Chanda ML, Graham AC, Topham L, Beggs S, Salter MW, Mogil JS (2011) Spinal cord Toll-like receptor 4 mediates inflammatory and neuropathic hypersensitivity in male but not female mice. *J Neurosci* 31:15450–15454.
- Su L, Wang C, Yu YH, Ren YY, Xie KL, Wang GL (2011) Role of TRPM8 in dorsal root ganglion in nerve injury-induced chronic pain. *BMC Neurosci* 12:120.
- Summer GJ, Romero-Sandoval EA, Bogen O, Dina OA, Khasar SG, Levine JD (2008) Proinflammatory cytokines mediating burn-injury pain. *Pain* 135:98–107.
- Sun JL, Xiao C, Lu B, Zhang J, Yuan XZ, Chen W, Yu LN, Zhang FJ, Chen G, Yan M (2013) CX3CL1/CX3CR1 regulates nerve injury-induced pain hypersensitivity through the ERK5 signaling pathway. *J Neurosci Res* 91:545–553.
- Taiwo YO, Levine JD (1989) Prostaglandin effects after elimination of indirect hyperalgesic mechanisms in the skin of the rat. *Brain Res* 492:397–399.
- Taiwo YO, Bjerknes LK, Goetzl EJ, Levine JD (1989) Mediation of primary afferent peripheral hyperalgesia by the cAMP second messenger system. *Neuroscience* 32:577–580.
- Tammi R, MacCallum D, Hascall VC, Pienimäki JP, Hyttinen M, Tammi M (1998) Hyaluronan bound to CD44 on keratinocytes is displaced by hyaluronan decasaccharides and not hexasaccharides. *J Biol Chem* 273:28878–28888.
- Tavianatou AG, Caon I, Franchi M, Piperigkou Z, Galesso D, Karamanos NK (2019) Hyaluronan: molecular size-dependent signaling and biological functions in inflammation and cancer. *FEBS J* 286:2883–2908.
- Taylor KR, Yamasaki K, Radek KA, Di Nardo A, Goodarzi H, Golenbock D, Beutler B, Gallo RL (2007) Recognition of hyaluronan released in sterile injury involves a unique receptor complex dependent on Toll-like receptor 4, CD44, and MD-2. *J Biol Chem* 282:18265–18275.
- Toole BP (2009) Hyaluronan-CD44 interactions in cancer: paradoxes and possibilities. *Clin Cancer Res* 15:7462–7468.
- Triantafyllidou K, Venetis G, Bika O (2013) Efficacy of hyaluronic acid injections in patients with osteoarthritis of the temporomandibular joint. A comparative study. *J Craniofac Surg* 24:2006–2009.
- Tuhkanen AL, Tammi M, Pelttari A, Agren UM, Tammi R (1998) Ultrastructural analysis of human epidermal CD44 reveals preferential distribution on plasma membrane domains facing the hyaluronan-rich matrix pouches. *J Histochem Cytochem* 46:241–248.
- Underhill C (1992) CD44: the hyaluronan receptor. *J Cell Sci* 103:293–298.
- Unsworth A, Dowson D, Wright V (1975) Some new evidence on human joint lubrication. *Ann Rheum Dis* 34:277–285.
- Vanhaesebroeck B, Guillermet-Guibert J, Graupera M, Bilanges B (2010) The emerging mechanisms of isoform-specific PI3K signalling. *Nat Rev Mol Cell Biol* 11:329–341.
- Vigetti D, Karousou E, Viola M, Deleonibus S, De Luca G, Passi A (2014) Hyaluronan: biosynthesis and signaling. *Biochim Biophys Acta* 1840:2452–2459.
- Wang Y, Abarbanell AM, Herrmann JL, Weil BR, Manukyan MC, Poynter JA, Meldrum DR (2010) TLR4 inhibits mesenchymal stem cell (MSC) STAT3 activation and thereby exerts deleterious effects on MSC-mediated cardioprotection. *PLoS One* 5:e14206.
- Wang Y, Su L, Morin MD, Jones BT, Whitby LR, Surakattula MM, Huang H, Shi H, Choi JH, Wang KW, Moresco EM, Berger M, Zhan X, Zhang H, Boger DL, Beutler B (2016) TLR4/MD-2 activation by a synthetic agonist with no similarity to LPS. *Proc Natl Acad Sci U S A* 113:E884–E893.
- Wight TN (2017) Provisional matrix: a role for versican and hyaluronan. *Matrix Biol* 60–61:38–56.
- Wight TN (2018) A role for proteoglycans in vascular disease. *Matrix Biol* 71–72:396–420.
- Woolf CJ, Ma Q (2007) Nociceptors—noxious stimulus detectors. *Neuron* 55:353–364.
- Wu PT, Kuo LC, Su FC, Chen SY, Hsu TI, Li CY, Tsai KJ, Jou IM (2017) High-molecular-weight hyaluronic acid attenuated matrix metalloproteinase-1 and -3 expression via CD44 in tendinopathy. *Sci Rep* 7:40840.
- Wu SC, Chen CH, Wang JY, Lin YS, Chang JK, Ho ML (2018) Hyaluronan size alters chondrogenesis of adipose-derived stem cells via the CD44/ERK/SOX-9 pathway. *Acta Biomater* 66:224–237.
- Yamawaki H, Hirohata S, Miyoshi T, Takahashi K, Ogawa H, Shinohata R, Demircan K, Kusachi S, Yamamoto K, Ninomiya Y (2009) Hyaluronan receptors involved in cytokine induction in monocytes. *Glycobiology* 19:83–92.
- Yang C, Cao M, Liu H, He Y, Xu J, Du Y, Liu Y, Wang W, Cui L, Hu J, Gao F (2012) The high and low molecular weight forms of hyaluronan have distinct effects on CD44 clustering. *J Biol Chem* 287:43094–43107.
- Yang Z, Qin W, Chen Y, Yuan B, Song X, Wang B, Shen F, Fu J, Wang H (2018) Cholesterol inhibits hepatocellular carcinoma invasion and metastasis by promoting CD44 localization in lipid rafts. *Cancer Lett* 429:66–77.
- Zhang Z, Qin P, Deng Y, Ma Z, Guo H, Guo H, Hou Y, Wang S, Zou W, Sun Y, Ma Y, Hou W (2018) The novel estrogenic receptor GPR30 alleviates ischemic injury by inhibiting TLR4-mediated microglial inflammation. *J Neuroinflammation* 15:206.